Self-Aligning Scanning Shack-Hartmann Sensor for Automatic Wavefront Measurements of High-NA Optics

Martin E. Fuerst, Nikolaus Berlakovich, Ernst Csencsics and Georg Schitter, *Senior Member, IEEE*
Christian Doppler Laboratory for Precision Engineering for Automated In-Line Metrology
Automation and Control Institute (ACIN), Technische Universität Wien
Vienna, Austria
martin.fuerst@tuwien.ac.at

***Abstract*—Optical parts, such as lenses or mirrors, are often qualified by surface shape metrology. Wavefront measurements allow for a more direct measurement of the performance of an optical part. However, the dynamic range of current wavefront sensors is not sufficient for measuring the wavefront generated by high-NA optical parts. In this paper, a wavefront sensor is combined with a mechatronic positioning system to overcome these limitations by repositioning and reorienting the wavefront sensor. Feedback loops are implemented to ensure a tangential orientation of the wavefront sensor in every measurement position. An experimental setup is constructed and a measurement strategy that compensates for tip and tilt between wavefront and sensor is developed. It is demonstrated that this setup is capable of directly measuring the wavefront of a high-NA optic.**

***Index Terms*—Shack-Hartmann wavefront sensor, Dynamic range extension, Optical metrology, Automatic optical inspection, Quality management**

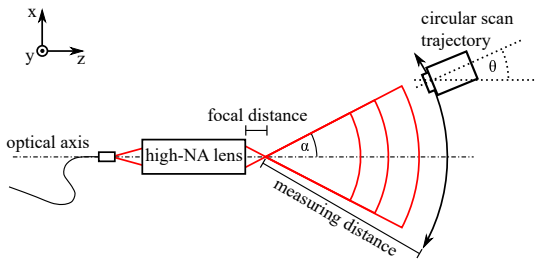

Fig. 1: Scanning wavefront sensor strategy. By increasing the measurement distance, the wavefront curvature is sufficiently reduced to be observable by the Shack-Hartmann sensor. To compensate the incidence angle, the sensor is reoriented (angle θ).

I. Introduction

An increasing number of industrial application depends on focused light, like laser material processing [1], advanced microscopy techniques or high-precision optical displacement sensing [2]. The technical quantity describing how strongly a lens can focus light is the numerical aperture (NA), defined as $NA = n \cdot \sin\alpha$ with n being the refractive index of the medium and α the half opening angle of the focused beam [3] (see also Fig. 1). The NA of an optical element is defined by the design of the component, but the quality of the focused spot can be degraded by aberrations, which are often caused by misalignments or manufacturing errors [4].

To minimize optical aberrations, optical component design moves from spherical parts, which are comparatively easy to manufacture and align [5], to aspherical parts and even freeform parts. While the quality of freeform parts is even more challenging to assess than the classical, spherical focusing optics, there is a mutual characteristic [6]: The qualification relies on *shape* measurements of the optical component, which are either collected by interferometric methods or by coordinate-measuring machines (CMMs).

Interferometric methods offer sub-nm resolution and are thus in widespread use for optical flats [7]. To measure highly divergent wavefronts, however, null-elements are required, which greatly reduce the universality of the measurement tool as each new surface geometry requires a new null-lens. Additionally, the null-optic is an additional source of uncertainty in the measurement process. Further, the interferometric approach suffers from a high vibration sensitivity, which renders it difficult to use it in industrial environments.

The CMM is well suited for nearly any part shape, can be equipped with tactile or non-tactile probes, and offers a nm-resolution comparable to the interferometric approach [8]. Optical parts are typically measured with non-tactile probes, as delicate coatings may be damaged by a tactile probe [9]. Compared to interferometric approaches, CMMs are typically much slower, as the surface data has to be acquired point-by-point or line-by-line.

To avoid the problems inherent to shape measurements, it was proposed to directly measure optical part *performance* [6]. This can be achieved by measuring the shape of the optical wavefront that is transmitted or reflected by an optical part or system. A commonly used wavefront sensor is the Shack-Hartmann sensor (SHS), which is a camera-based sensor that measures the shape of an incoming wavefront region in a single shot [10]. As Shack-Hartmann sensors are small, robust, fast and comparatively insensitive to vibrations, they are well

Pre-print version of the article: M. E. Fuerst, N. Berlakovich, E. Csencsics, and G. Schitter, "Self-Aligning Scanning Shack-Hartmann Sensor for Automatic Wavefront Measurements of High-NA Optics," *2020 IEEE International Instrumentation and Measurement Technology Conference*, 2020. DOI: 10.1109/I2MTC43012.2020.9128499

suited for industrial environments [11]. Their capability to characterize lenses bigger than the sensor aperture was recently demonstrated [12], [13]. This was done by manual, linear repositioning of the sensor and subsequent stitching of the acquired wavefront subaperture images. However, the Shack-Hartmann sensor is limited when it comes to the measurement of highly divergent wavefronts [14]. This is a problem when evaluating focusing optics, as these require high numerical apertures (NA) to create small, diffraction-limited focal spots. Approaches involving null-optics to enable Shack-Hartmann-wavefront sensing of high-NA lenses were also demonstrated, e.g. [15], but these suffer from the necessity of a specific null-optic and the additional uncertainties introduced by that element.

A recently published approach bypasses the limitations of the Shack-Hartmann sensor by mechanically repositioning the sensor along the wavefront [16]. The idea is to increase the measurement distance and thereby reduce the wavefront curvature incident on the sensor (see Fig. 1). In this case, only a part of the entire wavefront is observed in a single wavefront image, such that the sensor needs to be moved to multiple positions along the wavefront for collecting a number of partial images. The collected data is then interpreted in combination with the positioning data to obtain the complete wavefront. However, the setup presented in [16] is only partially automated, as the sensor positions and orientations are pre-planned based on the expected wavefront shape, limiting its applicability for arbitrary optics.

The contribution of this paper is the design and control of a fully automated scanning setup to directly measure the wavefront of a high-NA optical part. This is achieved by automatically planning a measurement trajectory from an inital alignment step, implementing feedback loops to orient the sensor tangentially to the wavefront under test and stitching the recorded subapertures together to form a representation of the global wavefront.

II. Shack-Hartmann wavefront sensing

A. Sensor principle

A Shack-Hartmann sensor consists of a microlens array and an image sensor [10]. The working principle is illustrated in Fig. 2a. Each microlens produces a focused spot on the image sensor, the position of the spot being dependent on the local slope of the wavefront incident on the microlens. From the recorded spot pattern, local slopes can be calculated via

$$\tan(\alpha) = \frac{\Delta x}{f_L} \tag{1}$$

with Δx the displacement of a spot from its reference position, f_L the focal length of the lenslet and α the wavefront slope (adapted from [17]). The local slope map is then used to reconstruct the wavefront shape [10]. Shack-Hartmann sensors offer a high measurement speed, are relatively robust to vibrations and have sub-wavelength resolution down to 0.01 λ [11].

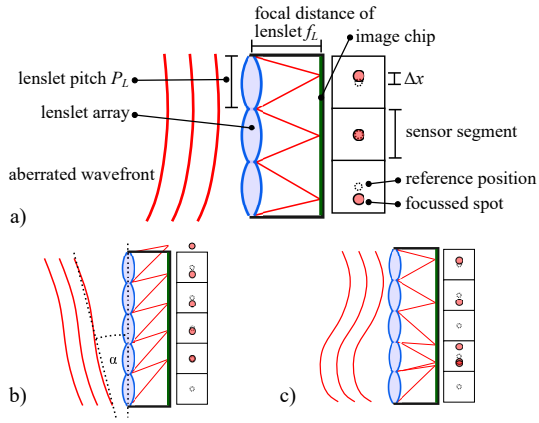

Fig. 2: Principle of a Shack-Hartmann sensor. a) Working principle and labeled components of a SHS. b) For a large global tilt of the incident wavefront, spots leave their assigned sensor regions. c) For large local curvature, multiple spots are registered in the same sensor region.

B. Limitations

Two wavefront characteristics limit the Shack-Hartmann sensor's dynamic range: wavefront slope and wavefront curvature [14].

Wavefront slope describes the average angle between incident wavefront and sensor aperture. If this angle is too large, the focused spots form outside their assigned regions on the sensor chip (see Fig. 2b)). To ensure that spots are registered within their respective sensor regions, the maximum admissible incidence angle is limited to

$$\alpha_{max} = \frac{P_L}{2 \cdot f_L} \tag{2}$$

(with lenslet pitch P_L as in Fig. 2a)). For typical Shack-Hartmann sensor parameters ($P_L = 100 - 200$ µm, $f_L = 3 - 10$ mm), α_{max} is only a few degrees (1-5°).

Wavefront curvature describes the local variation of wavefront slope. If the curvature is too high, multiple spots may be formed in the same segment of the sensor, making the assignment of spot to lenslet ambiguous (see Fig. 2c)). Efforts to solve this problem by advanced spot assignment algorithms have been reported, e.g. by [18]. These algorithms typically rely on prior knowledge of the main encountered aberrations and cannot compensate for the optical degradations that also accompany high curvatures and slopes incident on the sensor.

C. Scanning Shack-Hartmann Sensor

To perform a wavefront measurement on a highly-divergent optic without using a nullifying element (and thus avoiding additional cost, inconvenience and aberration), a scanning Shack-Hartmann sensor (scanning-SHS) system is proposed. The limitations of a static SHS, discussed in the previous section, can be avoided by increasing the measurement distance and scanning along the wavefront generated by the

Pre-print version of the article: M. E. Fuerst, N. Berlakovich, E. Csencsics, and G. Schitter, "Self-Aligning Scanning Shack-Hartmann Sensor for Automatic Wavefront Measurements of High-NA Optics," *2020 IEEE International Instrumentation and Measurement Technology Conference*, 2020. DOI: 10.1109/I2MTC43012.2020.9128499

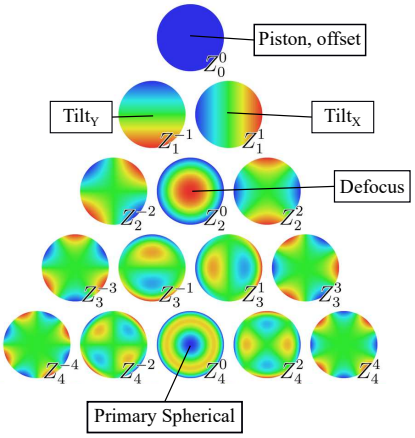

Fig. 3: First 15 Zernike polynomials and the related optical aberrations.

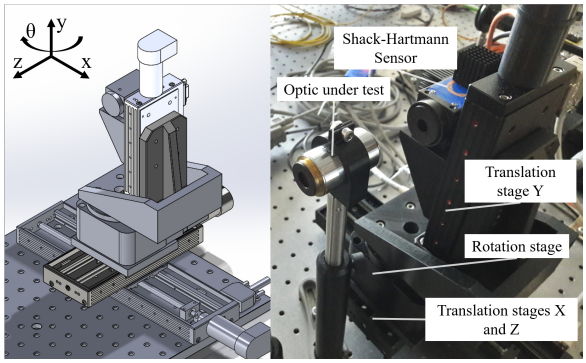

Fig. 4: The presented experimental setup as designed in SolidWorks and as constructed in the laboratory.

optic under test. Figure 1 illustrates the related tradeoffs. Increasing the distance reduces the curvature incident on the sensor aperture. However, to measure the complete wavefront, multiple measurements are now necessary. A pure translational scan perpendicular to the optical axis would result in high incidence angles at the outer positions, again exceeding the dynamic range of the Shack-Hartmann sensor. By reorienting the sensor tangentially to the wavefront, the incidence angle can be kept within limits. Effectively, the opening angle α is compensated by the stage angle θ.

D. Zernike decomposition

The so-called Zernike polynomials [19] are a set of base polynomials that are orthogonal on the unit disk. Any wavefront on a spherical aperture can thus be decomposed into its Zernike components. Their use is widespread in optics because the individual polynomials can be related to typical aberrations from optics theory, such as the Seidel aberrations. Figure 3 displays the first 15 Zernike polynomials Z_n^m in the standard ordering (by radial degree n and azimuthal degree m). The polynomials relevant for this paper are labeled accordingly.

III. Setup and Measurement Strategy

A. Experimental setup

To implement the scanning-SHS measurement system, an experimental automatic setup consisting of three translational stages and one rotational stage was designed. This four degree-of-freedom setup allows for scanning along an arbitrary trajectory in space, though the re-orientation of the sensor is limited to one degree of rotational freedom. Figure 4 shows the setup as designed in SolidWorks and as realized in the lab. The x-axis is mounted on the optical table, the z-axis is mounted on top of the x-axis. The rotation stage is mounted onto the x-z-stack and the y-stage is mounted on top of the rotation stage. The Shack-Hartmann sensor is mounted onto the y-stage. The rotational axis of the rotation stage is in the plane of the lenslet array of the Shack-Hartmann sensor.

The position-controlled linear stages (VT-80 stages from PI Physik Instrumente, Braunschweig, Germany) have a resolution of 500 nm and bidirectional repeatability of 10 µm. Maximum travel range in the X-, Y- and Z-direction is 200, 50 and 100 mm, respectively. For the highest divergent wavefront imaginable (opening angle of 180 degrees, NA = 1 in air), a half-circular trajectory with 100 mm radius could be scanned. The rotation stage (RM-3 model from Newmark Systems Inc., California) offers continuous rotation, a resolution of 0.29 arc seconds and a bidirectional repeatability of 45 arc seconds. The Shack-Hartmann Sensor (HR-2 model from Optocraft, Erlangen, Germany) has 85×53 lenslets arranged on a rectangular grid with 130 µm pitch. Its measurement rate is up to 20 Hz and it was calibrated in the factory for red light with the wavelength $\lambda = 635$ nm to offer an off-the-shelf resolution of $0.01\ \lambda$. Its focal length is 3.346 mm, suggesting a maximum incident wavefront angle of $1.13°$ (following Eq. 2). Through an advanced, proprietary spot-assignment algorithm, the sensor actually accepts angles up to $10°$, however, this is still insufficient for the high-NA optics modern high-performance applications require.

B. Measurement strategy

To automate the setup, the following measurement procedure is implemented (also illustrated in Fig. 5). First, the rotational stage is set to $0°$, so that the Shack-Hartmann sensor axis is roughly parallel to the optical axis of the system. Then, the sensor is automatically moved perpendicular to the optical axis in x-direction (refer to Fig. 4). After every step, a wavefront measurement is recorded and the $Tilt_X$ Zernike coefficient is extracted. From the size of this coefficient, the size and direction of the next step are calculated. This is repeated until the value of the $Tilt_X$-component is below the sensor noise. The same process is then repeated with the y-translation stage for the $Tilt_Y$-component.

After these steps, the sensor is positioned orthogonal to the wavefront, though not necessarily parallel to the optical axis of

Pre-print version of the article: M. E. Fuerst, N. Berlakovich, E. Csencsics, and G. Schitter, "Self-Aligning Scanning Shack-Hartmann Sensor for Automatic Wavefront Measurements of High-NA Optics," *2020 IEEE International Instrumentation and Measurement Technology Conference*, 2020. DOI: 10.1109/I2MTC43012.2020.9128499

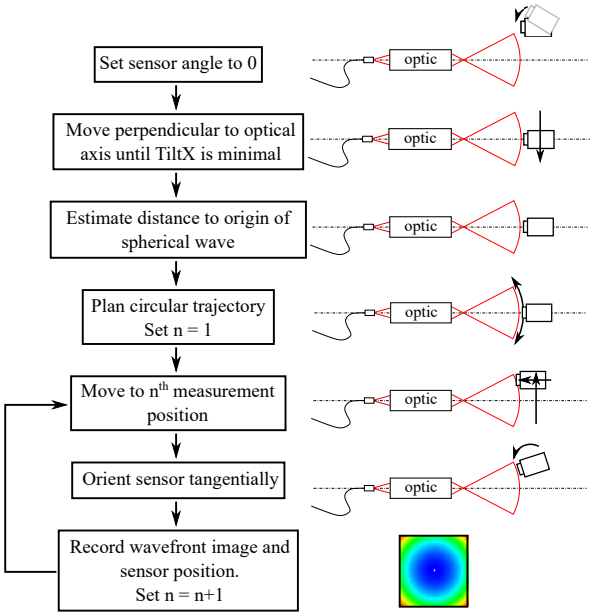

Fig. 5: Flowchart of the employed measurement strategy. After an initial rough alignment, a starting position is acquired, a trajectory is planned and in each measurement position, the sensor is automatically oriented tangentially to the wavefront.

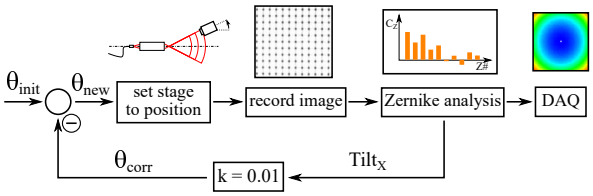

Fig. 6: Flowchart of the feedback loops employed in the measurement strategy. The recorded wavefront is decomposed into its constituent Zernike modes. The $Tilt_X$ component is then used to recalculate the desired θ-position.

the optic under test. In this position, another wavefront image is recorded and the wavefront radius r_{est} is calculated from the $Defocus$ Zernike coefficient. A circular scan trajectory is calculated from the estimated wavefront radius r_{est}, scan range θ_{max} and step size θ_{step}. The scan range is chosen to match the NA of the optic under test ($\theta_{max} = \arcsin(NA)$) and the step size is chosen to ensure an overlap region of about 50% between subsequent measurements.

$$\theta_i = -\theta_{max} + (i-1) \cdot \theta_{step} \tag{3a}$$
$$x_i = x_{init} - r_{est} \cdot \sin(\theta_i) \tag{3b}$$
$$y_i = y_{init} \tag{3c}$$
$$z_i = z_{init} + r_{est} \cdot (1 - \cos(\theta_i)) \tag{3d}$$

Then, the sensor is moved to one measurement position after the other and in each position, it is oriented tangentially to the wavefront by minimizing the $Tilt_X$- and $Tilt_Y$-components. This is achieved for $Tilt_X$ and $Tilt_Y$ in the same way, so it is exemplarily discussed in detail for $Tilt_X$ (see also Fig. 6). From the automatically preplanned trajectory, the rotational stage orients the sensor to an initial value $\theta_{init} = \theta_i$. A wavefront image is recorded and the $Tilt_X$ Zernike coefficient is extracted. The coefficient is multiplied by a factor k and subtracted from θ_{init}, resulting in θ_{new}. The rotational stage moves to θ_{new} and the process is repeated until the observed $Tilt_X$ is below the sensor noise. The factor k is determined in a preliminary experiment (data not shown) as the inverse value of the linear relation between positioning angle θ and observed $Tilt_X$ coefficient. The value for k was reduced by 30% to add a safety margin to avoid overshooting. The $Tilt_Y$ component is compensated in the same fashion as $Tilt_X$, but with the translation stage moving in y-direction.

In summary, this setup allows to automatically find and scan along the "equator" of any roughly spherical wavefront. For freeform optics, generating non-rotationally symmetric wavefronts, the setup can easily be extended to include a second rotational stage for full spherical scanning.

C. *Wavefront stitching*

With the setup, a number of wavefront images, referred to as *subapertures*, is recorded. As the sensor position is known for each subaperture, the wavefront data can be transformed to its corresponding position in a global laboratory system. Due to mechanical uncertainties and sensor misalignments, the subapertures might deviate from their correct positions causing errors in the wavefront reconstruction. To minimize the misalignments and reconstruct the wavefront, a stitching algorithm is used [20]. In this algorithm, an error function based on rigid body transformations is set up, which is minimized in order to correct the misalignments.

IV. Results and Discussion

A. *Repeatability of self-alignment*

To evaluate the mechanical stability of the scanning setup and the reliability of the feedback loops, measurements on a wavefront generated by an Olympus DPlan 10x microscope objective illuminated by the uncollimated end of a single-mode-fiber-coupled 635 nm laser diode were performed. The variation between the acquired subapertures was evaluated by comparing the Zernike components extracted from the subapertures for 100 runs. In each run, the sensor was moved along the same trajectory but self-aligned anew in each position. Figure 7 shows the results of these measurements. The uncertainties also already include the influences of the mechanical stage uncertainties. The variation in the low- and high-order Zernike coefficients is below the sensor resolution of 0.01 λ, which justifies the assumption that a repeatable wavefront measurement can be conducted after automated self-alignment.

Pre-print version of the article: M. E. Fuerst, N. Berlakovich, E. Csencsics, and G. Schitter, "Self-Aligning Scanning Shack-Hartmann Sensor for Automatic Wavefront Measurements of High-NA Optics," *2020 IEEE International Instrumentation and Measurement Technology Conference*, 2020. DOI: 10.1109/I2MTC43012.2020.9128499

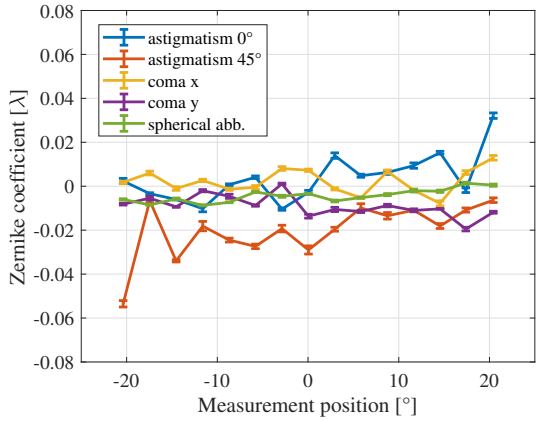

Fig. 7: Results of the repeatability measurements. Mean values and standard deviations of sub aperture Zernike coefficients over 100 runs are shown. The sensor was set to 15 positions on a circular trajectory from -21° to +21° degrees and automatically self-aligned in each position.

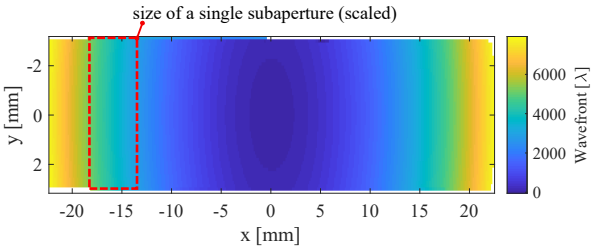

(a) Recorded and stitched high-NA wavefront.

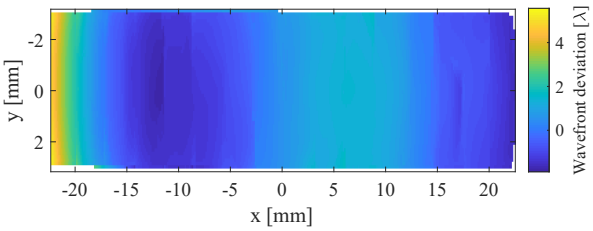

(b) Deviations from a fitted sphere.

Fig. 8: Result of an automatic wavefront measurement along a great circle. a) Stitched subapertures, the size of a single subaperture image is marked by a red rectangle. b) Remaining shape after subtraction of a fitted sphere.

B. Stitched high-NA wavefront

With the setup described in Section III, the wavefront created by a Motic 20x microscope objective (EC Plan, NA 0.45, corrected for infinity and 0.17 mm specimen cover glass) was investigated. The objective was illuminated by the collimated exit of a fiber-coupled 635 nm laser diode. A scan over the full opening angle of the objective (NA= 0.45 $\rightarrow \alpha = \pm 26.74°$) was performed in 15 steps.

Figure 8a displays the resulting stitched wavefront. The stitched wavefront was projected along the optical axis into the XY-plane to resemble the commonly used wavefront images of a single, static Shack-Hartmann sensor. The general wavefront shape matches the expectations and was automatically acquired and stitched even though the divergence of the wavefront exceeds the measurement range of the Shack-Hartmann sensor by far.

To evaluate the quality of an optic under test, the measured wavefront has to be compared to the desired or the design wavefront. For a focusing optic, such a reference wavefront closely resembles a sphere, therefore a sphere was fitted to the measurement data as a first reference. Figure 8b presents the deviations of the measured wavefront from the fitted sphere. The rms-deviation from the sphere is 1.32 λ or 0.84 µm.

C. Zernike reconstruction of global wavefront

The collected data can also be used to fit a global wavefront from Zernike polynomials. Figure 9a displays a 3D representation of the fitted wavefront. Figure 9b presents the Zernike coefficients that make up the wavefront shown in Fig. 9a. The $Tilt_X$- and $Tilt_Y$-components are close to zero while the $Defocus$-component is quite pronounced, as is expected from the focusing optic under test and the setup of the experiment. The higher-order aberrations are indicators for the quality of the optical component. The main components measured are $Vertical\ astigmatism$ (primary and secondary), $Vertical\ quadrafoil$ and $Primary\ spherical$ aberrations.

In summary, it is demonstrated that the fully automated, Self-Aligning Scanning Shack-Hartmann Sensor is capable of measuring a highly divergent wavefront by stitching a set of recorded subapertures, utilizing the positioning data, to represent the global wavefront, allowing further analysis such as a Zernike decomposition.

V. Conclusion

In this paper, a measurement system based on the concept of a Self-Aligning Scanning Shack-Hartmann Sensor was designed and implemented in order to obtain highly-divergent wavefronts. The repeatability of the self-alignment procedure was investigated, with the subaperture image uncertainties being within the range of the Shack-Hartmann sensor accuracy. The measurement of a wavefront with a numerical aperture of 0.45 (corresponding to an opening angle of $\pm$ 26°) was recorded by automatic repositioning and orienting of a Shack-Hartmann sensor and subsequent stitching of the individual subapertures.

Two ways of analyzing the resulting global wavefront image were investigated: Subtraction of a spherical reference surface from the measurement data and decomposition of the recorded surface into its Zernike components. Further research is primarily aimed at identifying the benefits and drawbacks of the evaluation strategies for different use cases. The comparison

Pre-print version of the article: M. E. Fuerst, N. Berlakovich, E. Csencsics, and G. Schitter, "Self-Aligning Scanning Shack-Hartmann Sensor for Automatic Wavefront Measurements of High-NA Optics," *2020 IEEE International Instrumentation and Measurement Technology Conference*, 2020. DOI: 10.1109/I2MTC43012.2020.9128499

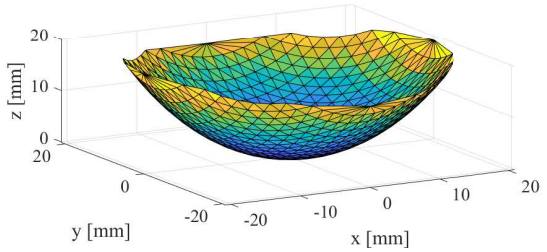

(a) 3D plot of a computed wavefront that fits the measurement data.

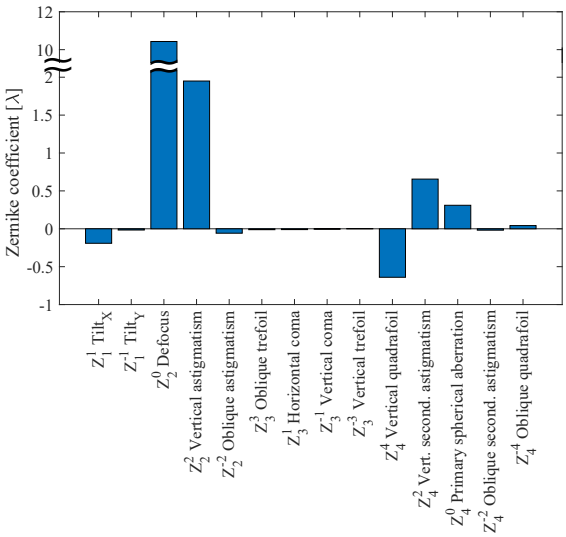

(b) Zernike coefficients of the reconstructed wavefront.

Fig. 9: A Zernike wavefront was fitted to the measurement data. a) 3D representation of the global wavefront. b) Zernike coefficients of the reconstructed wavefront.

with a reference surface is an indicator for optical component quality and may thus be used in manufacturing of optical elements while the Zernike decomposition can serve as an indicator for optical system alignment and may be employed in automatic alignment schemes.

Acknowledgment

The financial support by the Christian Doppler Research Association, the Austrian Federal Ministry for Digital and Economic Affairs, and the National Foundation for Research, Technology and Development, as well as MICRO-EPSILON MESSTECHNIK GmbH & Co. KG and ATENSOR Engineering and Technology Systems GmbH is gratefully acknowledged. We also want to thank Johannes Pfund and Ralf Dorn from Optocraft GmbH for their support and numerous colleagues from ACIN, especially Johannes Schlarp and Shingo Ito, for insightful discussions.

References

[1] J. D. Majumdar and I. Manna, "Laser material processing," *International Materials Reviews*, vol. 56, no. 5-6, pp. 341–388, nov 2011.

[2] X. Zou, X. Zhao, G. Li, Z. Li, and T. Sun, "Non-contact on-machine measurement using a chromatic confocal probe for an ultra-precision turning machine," *The International Journal of Advanced Manufacturing Technology*, vol. 90, no. 5-8, pp. 2163–2172, oct 2016.

[3] M. Born and E. Wolf, *Principles of optics: electromagnetic theory of propagation, interference and diffraction of light*. Elsevier, 2013.

[4] M. Scaggs and G. Haas, "Optical alignment influenced aberrations in laser beam delivery systems and their correction," in *Laser Resonators, Microresonators, and Beam Control XVII*, A. V. Kudryashov, A. H. Paxton, V. S. Ilchenko, L. Aschke, and K. Washio, Eds. SPIE, mar 2015.

[5] F. Lamontagne, U. Fuchs, M. Trabert, and A. Möhl, "Aspheric lens mounting," *International Optical Design Conference 2017*, vol. 57, no. 10, p. 7, 2017.

[6] F. Z. Fang, X. D. Zhang, A. Weckenmann, G. X. Zhang, and C. Evans, "Manufacturing and measurement of freeform optics," *CIRP Annals - Manufacturing Technology*, vol. 62, no. 2, pp. 823–846, 2013.

[7] B. C. Kim, T. Saiag, Q. Wang, J. Soons, R. S. Polvani, and U. Griesmann, "The Geometry Measuring Machine (GEMM) Project at NIST," *Proceedings of the 2004 ASPE Winter Top. Meeting, North Carolina, USA*, pp. 3–6, 2004.

[8] G. Dai and B. Sebastian, "A high precision micro / nano CMM using piezoresistive tactile probes," 2009.

[9] R. Henselmans, L. A. Cacace, G. F. Y. Kramer, P. C. J. N. Rosielle, and M. Steinbuch, "The NANOMEFOS non-contact measurement machine for freeform optics," *Precision Engineering*, vol. 35, no. 4, pp. 607–624, 2011.

[10] B. C. Platt and R. Shack, "History and Principles of Shack-Hartmann Wavefront Sensing," *Journal of Refractive Surgery*, vol. 17, no. 5, pp. S573–S577, 2001.

[11] M. Thier, R. Paris, T. Thurner, and G. Schitter, "Low-latency shack-hartmann wavefront sensor based on an industrial smart camera," *IEEE Transactions on Instrumentation and Measurement*, vol. 62, no. 5, pp. 1241–1249, 2013.

[12] D. R. Burada, K. K. Pant, M. Bichra, G. S. Khan, S. Sinzinger, and C. Shakher, "Experimental investigations on characterization of freeform wavefront using Shack–Hartmann sensor," *Optical Engineering*, vol. 56, no. 08, p. 1, 2017.

[13] K. K. Pant, D. R. Burada, M. Bichra, M. P. Singh, A. Ghosh, G. S. Khan, S. Sinzinger, and C. Shakher, "Subaperture stitching for measurement of freeform wavefront," *Applied Optics*, vol. 54, no. 34, p. 10022, 2015.

[14] M. Rocktäschel and H. J. Tiziani, "Limitations of the Shack-Hartmann sensor for testing optical aspherics," *Optics and Laser Technology*, vol. 34, no. 8, pp. 631–637, 2002.

[15] M. Fuerst, S. Unger, S. Ito, and G. Schitter, "Wavefront measurement based feedback control for automatic alignment of a high-NA optical system," *Journal of Physics: Conference Series*, vol. 1065, p. 032001, 2018.

[16] M. E. Fuerst and G. Schitter, "Scanning Wavefront Sensor for Measurement of Highly Divergent Wavefronts," *8th IFAC Symposium on Mechatronic Systems*, vol. 52, no. Mechatronics, pp. 25–30, 2019. [Online]. Available: https://doi.org/10.1016/j.ifacol.2019.11.644

[17] A. Chernyshov, U. Sterr, F. Riehle, J. Helmcke, and J. Pfund, "Calibration of a Shack-Hartmann sensor for absolute measurements of wavefronts," *Applied Optics*, vol. 44, no. 30, pp. 6419–6425, 2005.

[18] S. Mauch, S. Member, J. Reger, and S. Member, "Real-Time Spot Detection and Ordering for a Shack – Hartmann Wavefront Sensor With a Low-Cost FPGA," *IEEE Transactions on Instrumentation and Measurement*, vol. 63, no. 10, pp. 2379–2386, 2014.

[19] G. M. Dai, *Wavefront optics for vision correction Vol. 179*. Bellingham: SPIE press, 2008.

[20] K. K. Pant, D. R. Burada, A. Ghosh, G. S. Khan, and C. Shakher, "Improved subaperture stitching for the measurement of freeform wavefront," in *Optics InfoBase Conference Papers*, vol. Part F114-, 2018, pp. 2–3.

Pre-print version of the article: M. E. Fuerst, N. Berlakovich, E. Csencsics, and G. Schitter, "Self-Aligning Scanning Shack-Hartmann Sensor for Automatic Wavefront Measurements of High-NA Optics," *2020 IEEE International Instrumentation and Measurement Technology Conference*, 2020. DOI: 10.1109/I2MTC43012.2020.9128499